Breath-hold single-photon emission tomography and computed tomography for predicting residual pulmonary function in patients with lung cancer

Manabu Sudoh, MD,[a] Kazuhiro Ueda, MD,[a] Yoshikazu Kaneda, MD,[a] Jinbo Mitsutaka, MD,[a] Tao-Sheng Li, MD,[a] Kazuyoshi Suga, MD,[b] Yasuhiko Kawakami, MD,[b] and Kimikazu Hamano, MD[a]

M. Sudoh, J. Mitsutaka, K. Hamano, K. Ueda, Y. Kaneda (*left to right*)

Objective: We sought to evaluate the utility of integrated breath-hold single-photon emission tomography and computed tomography imaging compared with that of simple calculation with the lung segment–counting technique for predicting residual pulmonary function in patients undergoing surgical intervention for lung cancer.

Methods: A prospective series of 22 patients undergoing anatomic lung resection for cancer were enrolled in this study. Postoperative residual forced expiratory volume in 1 second was predicted by measuring the radioactivity counts of the affected lobes or segments to be resected within the entire lungs by placement of regions of interest on single-photon emission tomography and computed tomography images. Residual forced expiratory volume in 1 second was also estimated by using the segment-counting technique.

Results: Both predicted values agreed well with postoperative forced expiratory volume in 1 second. Although the residual forced expiratory volume in 1 second predicted by means of single-photon emission tomography and computed tomography correlated well with that predicted by using segment counting, the values were significantly underestimated by the segment-counting technique in 4 outliers with severe emphysema. There were 2 patients with borderline pulmonary functional reserve whose residual forced expiratory volume in 1 second values were predicted more accurately by means of single-photon emission tomography and computed tomography than by using segment counting.

Conclusion: Integrated breath-hold single-photon emission tomography and computed tomography images allow the accurate prediction of postoperative pulmonary function but without statistical superiority over the simple segment-counting technique. Further study of the usefulness of single-photon emission tomography and computed tomography in patients with severe emphysema and borderline lung function should prove valuable because the segment-counting technique underestimates pulmonary functional reserve in these patients.

From the Division of Thoracic Surgery, Department of Medical Bioregulation,[a] and the Division of Radiology, Department of Radiopathology and Science,[b] Yamaguchi University School of Medicine, Yamaguchi, Japan.

Received for publication July 26, 2005; revisions received Nov 20, 2005; accepted for publication Dec 22, 2005.

Address for reprints: Kazuhiro Ueda, MD, Division of Thoracic Surgery, Department of Medical Bioregulation, Yamaguchi University School of Medicine, 1-1-1 Minami-Kogushi, Ube, Yamaguchi, 755-8505, Japan (E-mail: kaueda@c-able.ne.jp).

J Thorac Cardiovasc Surg 2006;131:994-1001

0022-5223/$32.00

doi:10.1016/j.jtcvs.2005.12.038

For patients with primary lung cancer, surgical resection remains the only potentially curative option. However, chronic underlying lung diseases often limit operability. Because predicted pulmonary functional reserve is the most important determinant for the decision to perform pulmonary resection,[1-3] extensive effort has been made to accurately predict postoperative pulmonary function by using various diagnostic modalities. The simple lung segment–counting technique is widely used to estimate postoperative pulmonary function by counting the number of functioning segments that will be reserved and the number of those that will be resected.[4] However, this will provide an accurate prediction only if all the functioning segments are functioning equally preoperatively and postoperatively. For patients with heterogeneous lung diseases, Tc-99m–macroaggregated albumin per-

Abbreviations and Acronyms

CT = computed tomography
3D = Three-dimensional
FEV_1 = forced expiratory volume in 1 second
FEV_{1ppo} = predicted postoperative forced expiratory volume in 1 second
HU = Hounsfield units
LAA = low-attenuation area
ROI = region of interest
SPET = single-photon emission tomography

TABLE 1. Patient characteristics*

Age (y)	71 ± 7.5
Sex (male/female)	19/3
Pack-years smoked	57 ± 44
FEV_1 (L)	2.0 ± 0.62
FEV_1 (% predicted)	63.4 ± 11.9
Resection (lobectomy/segmentectomy)	15/7

Results are expressed as means ± standard deviation unless otherwise specified. The number of resected subsegments was 10.5 ± 4.3 for lobectomy and 6.0 ± 2.5 for segmentectomy. *FEV_1*, Forced expiratory volume in 1 second. *n = 22.

fusion single-photon emission tomography (SPET) has been widely used to evaluate regional lung function.[5-8] However, in standard non–breath-hold SPET, respiratory lung motion and cyclically varying lung volume changes during image acquisition degrade image sharpness and complicate accurate identification of the areas corresponding with the lobes or segments to be resected.

At our institute, to solve these problems on standard perfusion SPET, we have recently introduced breath-hold perfusion SPET images acquired with a triple-headed SPET system and a laser-light respiratory tracking device.[9-11] These images are also used for obtaining reliable integrated images with routine breath-hold computed tomography (CT) images.[10,11] We expect that these SPET and integrated images will help to predict postoperative pulmonary function by providing accurate assessment of perfusion impairment and correlation with lung anatomy and might be superior to the simple segment-counting technique for this prediction. We conducted this study to evaluate the feasibility of using these images to predict postoperative pulmonary function in patients with lung cancer by comparing them with the simple lung segment–counting technique.

Materials and Methods

Study Subjects

The subjects of this prospective study were 22 patients who underwent anatomic lung resection for cancer. All patients underwent a pulmonary function test, thin-slice high-resolution CT, and breath-hold perfusion SPET studies. The patients' characteristics are shown in Table 1. Nineteen patients had peripheral-type tumors, and 3 had central-type tumors. The CT images showed varying degrees of focal low-attenuation areas (LAAs) representative of emphysematous changes with or without bullae in all 22 patients. The number of resected subsegments was 10.5 ± 4.3 for lobectomy and 6.0 ± 2.5 for segmentectomy. All patients were informed about the research protocol, which was approved by our institutional review board.

Breath-hold Perfusion SPET

Breath-hold perfusion SPET images were obtained by using a triple-headed SPET unit (GCA 9300 A/PI; Toshiba Medical System, Tokyo, Japan) and a laser-light respiratory tracking device (AZ-733; Anzai Sogyo Co, Osaka, Japan). Each patient was placed in the supine position, as in CT scanning, and a laser-light reflex plate was attached to the thoracic or abdominal wall to show the maximum respiratory movement. The laser-light reflex system was connected to a physiologic respiratory tracking device, which was used to monitor respiratory motion on the time-distance curves. We then gave each patient an intravenous injection of 259 MBq (7 mCi) of macroaggregated albumin. Breath-hold image acquisition was intermittently repeated until 5 adequate projection data sets with the same respiratory dimension could be obtained. The maximum difference in respiratory dimension among the 5 projection data sets was only 2.2 ± 0.5 mm on average (range, 1.1-4.3 mm) in all patients. The total examination time for breath-hold SPET imaging ranged from 2 to 6 minutes (mean, 3.5 ± 1.6 minutes). Subsequently, standard non–breath-hold SPET images during rest breathing were acquired by using a step-and-shoot mode.

On the image workstation (GCA 9300 A/DI; Toshiba Medical System, Shibaura, Japan), breath-hold SPET images were reconstructed from every 4° projection of the 5 data sets. Standard non–breath-hold SPET images were reconstructed from every 6° projection. The lung contour was drawn at a threshold of 20% of the maximum radioactivity of the lungs in each patient.

CT Scan and Emphysema Index

CT scans were performed with a 4-detector-row CT scanner (Siemens Volume Zoom; Siemens-Asahi Medical Ltd, Tokyo, Japan). With the patient in the supine position, 3-mm-thick, high-resolution CT images covering the entire lung were obtained in a 512 × 512 matrix during deep inspiratory breath-hold by using 3-mm collimation, with a scan time of 1.0 seconds at 120 to 130 kVp and 220 to 230 mA. Transaxial CT images were reconstructed with the lung algorithm.

To evaluate the distribution and extent of emphysematous lung areas in each patient, we created volume-rendering 3-dimensional (3D) images of lung-volume, LAA, and density-masked images, which highlighted the lung areas with attenuation values of less than −910 Hounsfield units (HU), which were representative of emphysematous areas, by using imaging software (M900 QUADRA; Zio Soft K.K., Osaka, Japan). Threshold limits of −600 to −1024 HU were applied to segment the entire lungs and to exclude soft tissues surrounding the lung and the large vessels within the lung. On 3D LAA and density-masked images, emphysematous areas were visualized as red colors (Figure 1). 3D

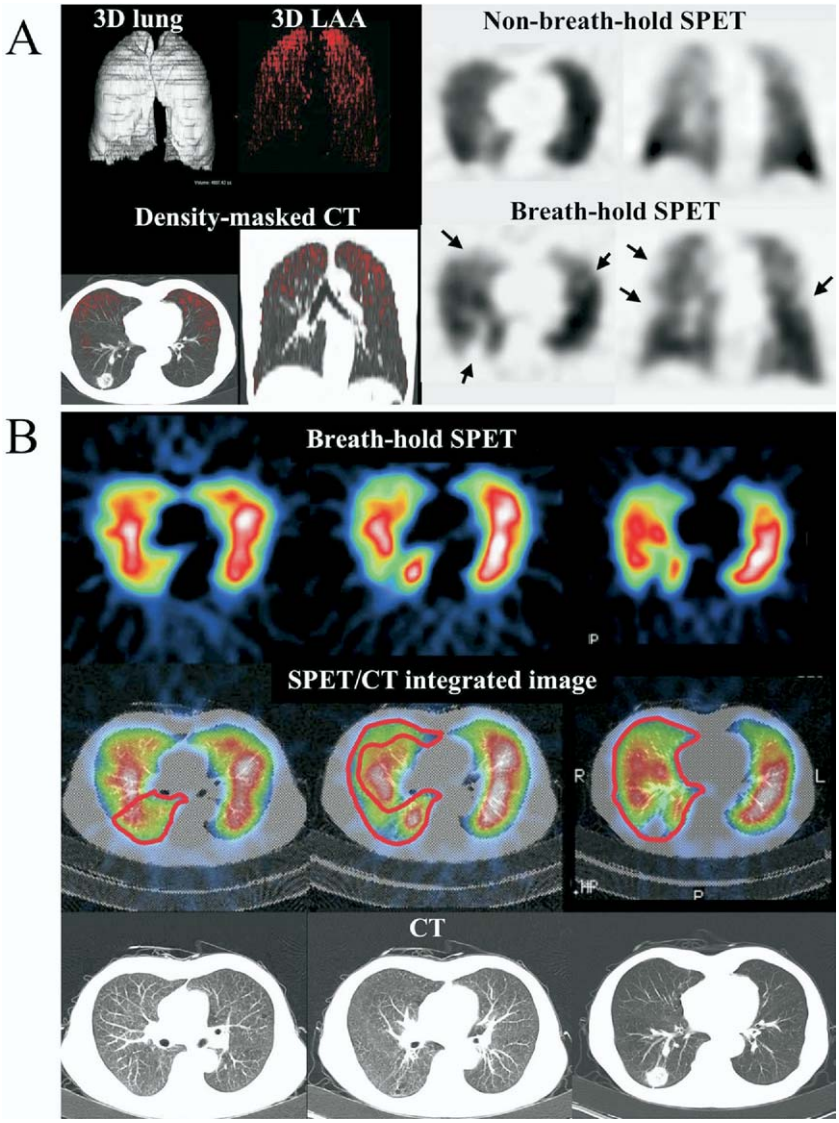

Figure 1. A, Three-dimensional *(3D)* lung volume and low-attenuation area *(LAA)* images (*top left*), density-masked computed tomographic *(CT)* image of the lung plane (*bottom left*), and breath-hold and standard non–breath-hold perfusion single-photon emission CT *(SPET)* images *(right)* in a 77-year-old man with adenocarcinoma in the right lower lobe and diffuse emphysema. The red areas on 3D LAA and density-masked CT images represent the distribution of emphysematous areas with CT attenuation values of less than −910 HU. The 3D LAA and density-masked CT images *(left)* clearly show that this patient has a moderate extent of focal emphysema, with an emphysema index of 18.2%, and a forced expiratory volume in 1 second *(FEV_1)* of 2.64 L. Although heterogeneous perfusion defects were seen on breath-hold and non–breath-hold images at the same transaxial lung plane as in the CT image and in the coronal dorsal lung plane, some defects were more distinct on the breath-hold images (*right, arrows*). Breath-hold SPET images showed extended perfusion defects at normal lung areas without LAAs. B, Image set of transaxial breath-hold SPET, SPET/CT integrated, and CT images. For regions of interest *(ROI)* placement *(red solid lines)* to predict postoperative FEV_1 after right middle and lower lobectomy, individual lung lobe borders could be outlined comprehensively by referring to the integrated images, although the borders were unclear on SPET images alone. In this patient the predicted FEV_1 of 1.96 L provided on the basis of integrated images was correlated better with the postoperative actual FEV_1 of 1.98 L than the predicted value of 1.63 L determined by means of lung segment counting.

lung volume images represent lung contours and volumes. By using 3D LAA and lung volume images, the area of emphysema was quantified by using the emphysema index: percentage of the number of voxels with attenuation values of less than −910 HU to the total number of voxels in the entire lungs.[12-16]

Integrated Breath-hold Perfusion SPET/CT Images

For the image integration of breath-hold SPET and CT images, DICOM data were electronically transferred to the teleradiologic workstation monitor (GMS 5500 A/DI, Toshiba Medical) and reformatted to a 168 × 168 matrix. Image integration was done with fully automated 3D multi-image registration software (automatic registration tool, Toshiba Medical).[10,11] The automated image integration was performed by definition of body contour and clustering of the voxels inside the body contour into a set of connected components by using a rigid body transformation technique. CT images were presented on a gray scale and SPET images were presented on a color scale to distinguish CT from SPET information on integrated images. The gray and color scales could be freely changed for adequate observations. The image integration process was completed within 1 to 2.5 minutes.

Image Interpretation and Data Analysis

Two independent observers (Y.K. and K.S.) with more than 6 years' experience in chest nuclear medicine counted the numbers of defects in all patients to compare the detectability of perfusion defects between breath-hold and standard non–breath-hold SPET images. Only well-defined defects were counted, and if there was inconsistency between the 2 observers, it was judged as a negative defect. For quantitative analysis, regions of interest (ROIs) were manually placed over relatively small defects and the surrounding

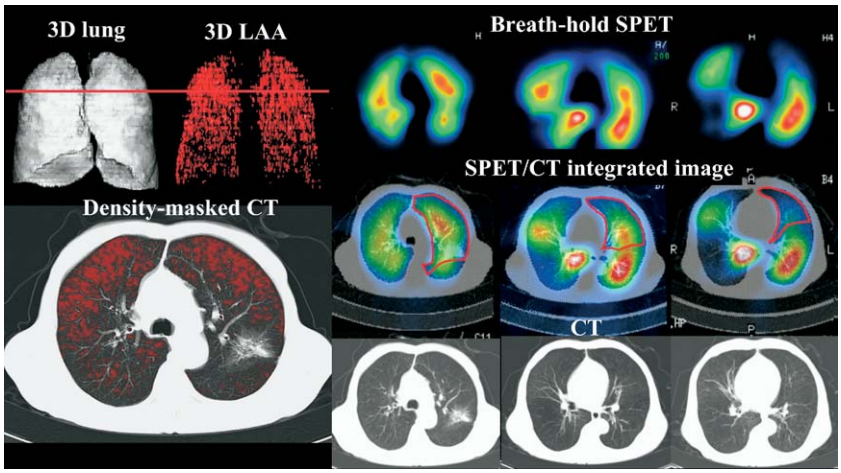

Figure 2. Three-dimensional *(3D)* lung volume and low-attenuation area *(LAA)* images (*top left*), density-masked computed tomographic *(CT)* image at the lung plane with primary lung cancer (*top left, red line*; *bottom left*), and image set of transaxial breath-hold perfusion single-photon emission CT *(SPET)*, SPET/CT integrated, and CT images *(right)* in a 69-year-old man with adenocarcinoma in the left upper lobe. The 3D LAA and density-masked CT images clearly show that this patient has severe diffuse emphysema, with an emphysema index of 28.7% and an FEV_1 of 0.91 L. The integrated images provided accurate ROI placement *(red solid lines)* for predicting the postoperative FEV_1 after left upper lobectomy. The predicted FEV_1 value of 0.76 L determined on the basis of the integrated images was marginal for lobectomy and correlated better with the postoperative actual FEV_1 of 1.19 L than the significantly underestimated predicted value of 0.69 L determined by means of lung segment counting.

GTS

normal areas, and the lesion–to–normal lung count ratios were calculated on the basis of the mean radioactivity per pixel for each ROI. The sizes of these ROIs ranged from 12 to 34 pixels (mean, 28 ± 14 pixels).

ROIs were placed over the lung areas to be resected by referring to integrated images to evaluate the contribution of integrated breath-hold SPET/CT images in the prediction of postoperative pulmonary function (Figure 1). Postoperative pulmonary function was predicted by using the following equation:

$$FEV_{1ppo} = Preoperative\ FEV_1 \times (Total\ lung\ radioactivity - Summed\ radioactivity\ of\ each\ ROI)/Total\ lung\ radioactivity$$ [5-7]

Postoperative pulmonary function was also predicted by means of a simple calculation with lung subsegment counting, as described by Nakahara and colleagues,[4] as follows: $FEV_{1ppo} = FEV_1(1 - [b - n]/[42 - n])$ where n is the number of obstructed subsegments, and b is the total number of removed subsegments. The total number of pulmonary subsegments was 42, with 10 each in the left upper lobe and left lower lobe, 6 in the right upper lobe, 4 in the right middle lobe, and 12 in the right lower lobe. The n value was calculated from the findings of preoperative fiberbronchoscopy or CT. The FEV_{1ppo} values were compared with actual postoperative values measured 3 to 4 months after the operation.

Statistical Analysis

The unpaired Student *t* test was used to test relations between categoric variables and numeric variables, and simple regression analysis was used to test relations between numeric variables.

Results

Breath-hold SPET images enhanced perfusion defect clarity and detected 46 (26%) additional defects (221 vs 175) compared with standard non–breath-hold images. The lesion-to-normal lung count ratios in the total 81 perfusion defects on breath-hold images were significantly lower than those on standard images (0.22 ± 0.16 vs 0.28 ± 0.19, $P < .001$).

The use of SPET/CT integrated images allowed comprehensive ROI placement over the lung areas to be resected in all patients (Figures 1-3). The FEV_{1ppo} estimated on the basis of integrated images was 1.66 ± 0.5 L, and the linear correlation coefficient with postoperative actual FEV_1 was 0.914 ($P < .0001$, Table 2). The FEV_{1ppo} estimated by means of segment counting was 1.59 ± 0.5 L, and the linear correlation coefficient with postoperative FEV_1 was 0.911 ($P < .0001$, Table 2). Both the FEV_{1ppo} estimated on the basis of integrated images and the FEV_{1ppo} estimated by means of segment counting were significantly lower than postoperative actual FEV_1 (1.83 ± 0.6 L, both $P < .01$). The FEV_{1ppo} values estimated on the basis of integrated images and segment counting were well correlated (correlation coefficient = 0.962, Table 2), with the exception of 4 outliers, which had differences of more than 10% of FEV_{1ppo} estimated by means of segment counting (Figure 4). In these outliers FEV_{1ppo} estimated on the basis of integrated images (1.64 ± 0.6 L) agreed well with postoperative actual FEV_1 (1.68 ± 0.4 L), although the values were underestimated by using the segment-counting technique (1.35 ± 0.5 L). In these outliers the area of emphysema on density-masked CT images was significantly higher than that in the remaining 18 patients (26% ± 6.3% vs 8% ± 6.1%, $P < .001$). There were 2 patients with borderline operative pulmonary function as a result of emphysema. Initially, we planned to perform a left upper lobectomy in both patients to resect the primary tumor. In one patient the FEV_{1ppo} values as estimated on the basis of segment counting and integrated

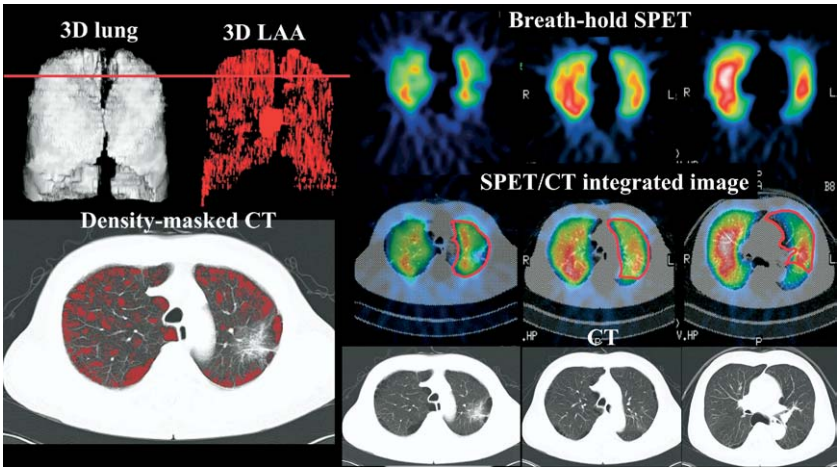

Figure 3. Three-dimensional *(3D)* lung volume and low-attenuation area *(LAA)* images (*left*; *top*), density-masked computed tomographic *(CT)* image at the lung plane with primary lung cancer (*top left*, *red line*; *bottom left*), and image set of transaxial breath-hold perfusion single-photon emission CT *(SPET)*, SPET/CT integrated, and CT images *(right)* in a 68-year-old man with adenocarcinoma in left upper lobe. The 3D LAA and density-masked CT images clearly show that this patient has bullous emphysema, with an emphysema index of 15.2% and an FEV_1 of 0.97 L. The predicted residual FEV_1 values after left upper lobectomy on the basis of lung segment counting and integrated images were 0.71 L and 0.62 L, respectively. Based on the marginal FEV_1 predicted on the basis of integrated images, this patient was recommended to undergo resection of the left upper segment (S^{1+2} and S^3). By preserving the left lingular segment, the residual FEV_1 values predicted by means of lung segment counting and integrated images were 0.82 L and 0.74 L, respectively. The predicted FEV_1 determined on the basis of integrated images correlated better with the postoperative actual FEV_1 of 0.71 L than the predicted value provided by means of lung segment counting.

images were 0.69 L and 0.76 L, respectively. Postoperatively, this patient recovered without any cardiopulmonary complications, and the FEV_{1ppo} as estimated on the basis of integrated images was closer to the measured value (1.19 L) than the FEV_{1ppo} as estimated by means of segment counting (Figure 2). In the other patient the FEV_{1ppo} values as estimated on the basis of segment counting and integrated images were 0.74 L and 0.62 L, respectively. On the basis of the limited FEV_{1ppo} as estimated on the basis of integrated images, we recommended to the patient that he undergo resection of the left upper segment (S^{1+2} and S^3). By preserving the left lingular segment, the FEV_{1ppo} values as estimated on the basis of segment counting and integrated images were 0.82 L and 0.74 L, respectively. Postoperatively, the patient remained free of cardiopulmonary complications, and the actual FEV_1 (0.71 L) correlated well with the FEV_{1ppo} as estimated on the basis of integrated images (Figure 3).

TABLE 2. The linear correlation coefficient for the variables shown

Variables	Coefficient	*P* value
$FEV_{1ppo,\ SPET/CT} \times FEV_{1,\ postoperative}$	0.914	<.0001
$FEV_{1ppo,\ segment} \times FEV_{1,\ postoperative}$	0.911	<.0001
$FEV_{1ppo,\ SPET/CT} \times FEV_{1ppo,\ segment}$	0.962	<.0001

FEV_1, Forced expiratory volume in 1 second; *FEV_{1ppo}*, predicted postoperative FEV_1; *$FEV_{1ppo,\ SPET/CT}$*, FEV_{1ppo} estimated by means of single-photon emission tomography/computed tomography; *$FEV_{1ppo,\ segment}$*, FEV_{1ppo} estimated by means of segment counting; *$FEV_{1,\ postoperative}$*, FEV_1 measured postoperatively.

Discussion

Although perfusion SPET is widely used to evaluate functional reserve after pulmonary resection,[5-8] it has some limitations. Respiratory motion during image acquisition degrades image clarity and compromises the detection of ill-defined perfusion defects. Moreover, there is no detailed anatomic landmarks on SPET images, resulting in large interobserver variability in estimating the functional contribution of specific lung areas. Conversely, the present breath-hold SPET images and integrated images with CT are refined images that have been developed to solve these problems. In the present study breath-hold SPET images enhanced the image clarity of perfusion defects and detected defects more sensitively than standard non–breath-hold images. The reliable integrated images with CT images allowed accurate outlining of the lung lobes and segments to be resected for ROI analysis. Although the superiority of these integrated images over the simple segment-counting technique in predicting postoperative FEV_1 did not reach significance in this study, we were able to use these images to accurately predict the values in 4 outliers with severe emphysema. In these outliers the segment-counting technique significantly underestimated the values. These integrated images might especially contribute to accurate prediction of postoperative pulmonary function in patients with severe emphysema.

To date, pulmonary perfusion SPET/CT integrated images have not been widely used because of the difficulty in obtaining reliable image integration. However, the present breath-hold SPET images can provide reliable integrated

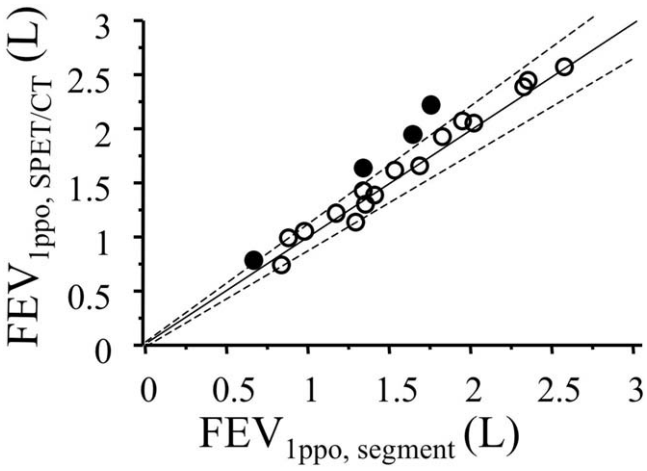

Figure 4. Linear dependence between the postoperative predicted forced expiratory volume in 1 second *(FEV_{1ppo})* estimated on the basis of single-photon emission tomography and computed tomography *(SPET/CT)* integrated images and the FEV_{1ppo} estimated by means of the segment-counting method. Both values were closely dependent (correlation coefficient = 0.962) in all patients, except for 4 outliers *(filled circles)* whose residual pulmonary function was underestimated by means of the segment-counting method. The *solid line* expresses y = x, and the *dotted lines* express y = 0.9 x and y = 1.1 x.

images with CT images at the same deep inspiratory phase. In our preliminary study the integrated images of the same respiratory-phase SPET and CT images have allowed comprehensive outlining of the lung lobes to be resected, yielding a better prediction of postoperative pulmonary function compared with SPET images alone, with excellent interobserver reproducibility.[11] In the present study the deep respiratory breath-hold SPET/CT integrated images also allowed us to accurately outline the areas to be resected, even in patients undergoing segmental lung resection. With the increasing incidence of peripheral small adenocarcinoma, segmentectomy might become the treatment of choice.[17-21] We expect that the present integrated images will become a more attractive tool for identifying pulmonary functional reserve in patients undergoing this type of operation for limited function.

The area of emphysema quantified by means of CT, but not preoperative FEV_1, was significantly associated with the discrepancy between FEV_{1ppo} estimated on the basis of integrated images and FEV_{1ppo} estimated by means of segment counting. This might assist in the selection of patients who should be considered for integrated images by providing an accurate prediction of postoperative respiratory function. Because FEV_1 of less than 700 mL is reported to be associated with a significantly higher mortality risk,[1-3] the minimal disagreement between the 2 predicted values is critical for the determination of operability in patients with borderline function. In our series there were 2 patients with borderline function caused by severe emphysema. SPET/CT integrated images helped to verify operability in one patient with an FEV_{1ppo} of less than 700 mL as estimated by means of segment counting (Figure 2). These integrated images also suggested that the change in the operative method was appropriate in the other patient with an FEV_{1ppo} of more than 700 mL as estimated by means of segment counting (Figure 3). Integrated images contributed greatly to predict postoperative functional reserve more accurately than segment counting in both these patients, who recovered postoperatively without any cardiopulmonary complications. Thus in patients with severe emphysema and borderline function, assessment of perfusion impairment with integrated images appears indispensable for determining operability.

Breath-hold perfusion SPET images showed more extended perfusion defects compared with LAAs depicted by using density-masked CT in our patients, with occasional perfusion defects at normal lung areas without LAAs (Figure 1). The superiority of perfusion SPET in detection of emphysematous lungs was also demonstrated by a previous animal study.[22] Perfusion defects at normal lung areas on CT images were also documented in patients with pulmonary emphysema in previous clinical studies by us and others.[23-26] Smoking-induced mild inflammatory changes in airways, alveolar destruction, or both are not well identified on CT images because of the limitation of spatial resolution. Even in cases without focal alveolar destruction LAAs, smoking-induced airflow obstruction in central-peripheral airways should impair regional perfusion considerably. Breath-hold perfusion SPET images, which enhance the detectability of perfusion defects, seem to further facilitate the advantage of SPET study in the detection of smoking-induced lung pathology.

Regardless of the good correlation between FEV_{1ppo} values estimated on the basis of SPET/CT integrated images and values measured postoperatively in our patients, the predicted FEV_1 values were significantly lower than postoperative FEV_1 values. Postoperative pulmonary function can be underestimated because pulmonary resection itself sometimes results in improved residual lung function in patients with emphysema. Relief of airflow obstruction, improved respiratory muscle function and elimination of dead space ventilation in ventilated but unperfused areas, and improved cardiovascular hemodynamics might all contribute to this unexpected improvement.[16,27-29] Some mathematic correction with variables such as the area of emphysema might be required for obtaining more accurate prediction. Further study on a larger patient population is warranted to solve this issue.

In the present study we focused on the estimation of FEV_{1ppo} because residual FEV_1 is the most relevant indicator of morbidity and mortality after major pulmonary resection among all pulmonary functional variables. Likely to the estimation of residual FEV_1, both the segment-counting technique and integrated images accurately estimated postoperative vital capacity ($r = 0.879$ for segment counting and $r = 0.863$ for integrated images) and postoperative diffusing capacity for carbon monoxide ($r = 0.961$ for segment counting and $r = 0.960$ for integrated images). In contrast, unlikely to the estimation of residual FEV_1, postoperatively measured vital capacity and diffusing capacity for carbon monoxide were not significantly better than the estimated residual values (all $P > .05$, paired t test). These results might support the notion that residual FEV_1 values are likely to be affected by a volume-reduction effect compared with vital capacity and diffusing capacity, especially for patients with emphysema.

In summary, breath-hold perfusion SPET images enhanced perfusion defect clarity and detected perfusion defects more sensitively than standard images and also provided reliable integrated images with the same respiratory-phase CT images. The reliable SPET/CT integrated images helped to accurately outline the lung lobes or segments to be resected for ROI analysis. Although the superiority of this method over simple lung segment counting for prediction of postoperative pulmonary function was not demonstrated statistically in this study population, our results indicate that patients with severe emphysema and borderline pulmonary function should be evaluated with SPET/CT integrated images for accurate prediction of postoperative pulmonary function because the simple segment-counting technique appears to inherently underestimate functional reserve in these patients.

References

1. Markos J, Mullan BP, Hillman DR, Musk AW, Antico VF, Lovegrove FT, et al. Preoperative assessment as a predictor of mortality and morbidity after lung resection. *Am Rev Respir Dis.* 1989;139:902-10.
2. Kearney DJ, Lee TH, Reilly JJ, DeCamp MM, Sugarbaker DJ. Assessment of operative risk in patients undergoing lung resection. Importance of predicted pulmonary function. *Chest.* 1994;105:753-9.
3. Brunelli A, Al Refai M, Monteverde M, Sabbatini A, Xiume F, Fianchini A. Predictors of early morbidity after major lung resection in patients with and without airflow limitation. *Ann Thorac Surg.* 2002; 74:999-1003.
4. Nakahara K, Monden Y, Ohno K, Miyoshi S, Maeda H, Kawashima Y. A method for predicting postoperative lung function and its relation to postoperative complications in patients with lung cancer. *Ann Thorac Surg.* 1985;39:260-5.
5. Hirose Y, Imaeda T, Doi H, Kokubo M, Sakai S, Hirose H. Lung perfusion SPECT in predicting postoperative pulmonary function in lung cancer. *Ann Nucl Med.* 1993;7:123-6.
6. Petersson J, Sanchez-Crespo A, Rohdin M, Montmerle S, Nyren S, Jacobsson H, et al. Physiological evaluation of a new quantitative SPECT method measuring regional ventilation and perfusion. *J Appl Physiol.* 2004;96:1127-36.
7. Imaeda T, Kanematsu M, Asada S, Seki M, Matsui E, Doi H, et al. Prediction of pulmonary function after resection of primary lung cancer—utility of inhalation-perfusion SPECT imaging. *Clin Nucl Med.* 1995;20:792-9.
8. Piai DB, Quagliatto R Jr, Toro I, Cunha Neto C, Etchbehere E, Camargo E. The use of SPECT in preoperative assessment of patients with lung cancer. *Eur Respir J.* 2004;24:258-62.
9. Suga K, Kawakami Y, Zaki M, Yamashita T, Matsumoto T, Matsunaga N. Pulmonary perfusion assessment with respiratory gated 99mTc macroaggregated albumin SPECT: preliminary results. *Nucl Med Commun.* 2004;25:183-93.
10. Suga K, Yasuhiko K, Zaki M, Yamashita T, Seto A, Matsumoto T, et al. Assessment of regional lung functional impairment with co-registered respiratory-gated ventilation/perfusion SPET-CT images: initial experiences. *Eur J Nucl Med Mol Imaging.* 2004;31: 240-9.
11. Suga K, Kawakami Y, Zaki M, Yamashita T, Shimizu K, Matsunaga N. Clinical utility of co-registered respiratory-gated ^{99m}Tc-Tecnegas/MAA SPECT-CT images in the assessment of regional lung functional impairment in patients with lung cancer. *Eur J Nucl Med Mol Imaging.* 2004;31:1280-90.
12. Park KJ, Bergin CJ, Clausen JL. Quantitation of emphysema with three-dimensional CT densitometry: comparison with two-dimensional analysis, visual emphysema scores, and pulmonary function test results. *Radiology.* 1999;211:541-7.
13. Kinsella M, Muller NL, Abboud RT, Morrison NJ, DyBuncio A. Quantitation of emphysema by computed tomography using a "density mask" program and correlation with pulmonary function tests. *Chest.* 1990;97:315-21.
14. Lamers RJ, Thelissen GR, Kessels AG, Wouters EF, van Engelshoven JM. Chronic obstructive pulmonary disease: evaluation with spirometrically controlled CT lung densitometry. *Radiology.* 1994;193:109-13.
15. Knudson RJ, Standen JR, Kaltenborn WT, Knudson DE, Rehm K, Habib MP, et al. Expiratory computed tomography for assessment of suspected pulmonary emphysema. *Chest.* 1991;99:1357-66.
16. Vesselle H. Functional imaging before pulmonary resection. *Semin Thorac Cardiovasc Surg.* 2001;13:126-36.
17. Watanabe T, Okada A, Imakiire T, Koike T, Hirono T. Intentional limited resection for small peripheral lung cancer based on intraoperative pathologic exploration. *Jpn J Thorac Cardiovasc Surg.* 2005;53: 29-35.
18. Okada M, Nishio W, Sakamoto T, Uchino K, Yuki T, Nakagawa A, et al. Effect of tumor size on prognosis in patients with non-small cell lung cancer: the role of segmentectomy as a type of lesser resection. *J Thorac Cardiovasc Surg.* 2005;129:87-93.
19. Koike T, Yamato Y, Yoshiya K, Shimoyama T, Suzuki R. Intentional limited pulmonary resection for peripheral T1 N0 M0 small-sized lung cancer. *J Thorac Cardiovasc Surg.* 2003;125:924-8.
20. Kodama K, Doi O, Higashiyama M, Yokouchi H. Intentional limited resection for selected patients with T1 N0 M0 non-small-cell lung cancer: a single-institution study. *J Thorac Cardiovasc Surg.* 1997; 114:347-53.
21. Yoshikawa K, Tsubota N, Kodama K, Ayabe H, Taki T, Mori T. Prospective study of extended segmentectomy for small lung tumors: the final report. *Ann Thorac Surg.* 2002;73:1055-8.
22. Noma S, Moskowitz GW, Herman PG. Pulmonary scintigraphy in elastase-induced emphysema in pigs. Correlation with high-resolution computed tomography and histology. *Invest Radiol.* 1992;27:429-35.
23. Jamader DA, Kazerooni EA, Martinez FJ, Wahl RL. Semi-quantitative ventilation/perfusion scintigraphy and single-photon emission tomography for evaluation of lung volume reduction surgery candidates: description and prediction of clinical outcome. *Eur J Nucl Med.* 1999;26:734-42.
24. Suga K, Nishigauchi K, Matsunaga N, Kawakami Y, Kume N, Sugi K, et al. Three-dimensional surface displays of perfusion SPECT in the evaluation of patients with pulmonary emphysema for thoracoscopic lung volume reduction surgery. *Nucl Med Commun.* 1997; 18:719-27.
25. Muller NL, Coxson H. Chronic obstructive pulmonary disease. 4: imaging the lungs in patients with chronic obstructive pulmonary disease. *Thorax.* 2005;57:982-5.

26. Miller RP, Muller NL, Vedal S. Limitations of computed tomography in the assessment of emphysema. *Am Rev Respir Dis.* 1989; 139:980-3.
27. Jubran A, Laghi F, Mazur M, Parthasarathy S, Garrity ER Jr, Fahey PJ, et al. Partitioning of lung and chest-wall mechanics before and after lung volume reduction surgery. *Am J Respir Crit Care Med.* 1998; 158:306-10.
28. Sciurba FC, Rogers RM, Keenan RJ, Slivka WA, Gorcsan J 3rd, Ferson PF, et al. Improvement in pulmonary function and elastic recoil after lung-reduction surgery for diffuse emphysema. *N Engl J Med.* 1996;334:1095-9.
29. Laghi F, Jubran A, Topeli A, Fahey PJ, Garrity ER Jr, de Pinto DJ, et al. Effect of lung volume reduction surgery on diaphragmatic neuromechanical coupling at 2 years. *Chest.* 2004;125:2188-95.